2020 IEEE/RSJ International Conference on Intelligent Robots and Systems (IROS)
October 25-29, 2020, Las Vegas, NV, USA (Virtual)

Design and Modeling of a Parallel Shifted-Routing Cable-Driven Continuum Manipulator for Endometrial Regeneration Surgery

Jianhua Li, Student Member, IEEE, Yuanyuan Zhou, Jichun Tan, Zhidong Wang, Senior Member, IEEE, and Hao Liu, Member, IEEE

***Abstract*—Endometrial regeneration surgery is a new therapy for intrauterine adhesion (IUA). However, existing instruments lacking dexterity and compliance are with difficulty to successfully perform the tasks of generating transplant wounds and transplanting stem cells during endometrial regeneration surgery. This paper presents a novel shifted-routing continuum manipulator which is driven by only two cables but has high dexterity, simple structure and small size. The design of the continuum manipulator with novel actuation strategy is introduced and the manipulator's kinematic model is also derived. The analysis and simulation imply that shifted-routing strategy improves the dexterity of manipulators under limited actuation numbers and enhances the ability of reaching targets on fundus and corpus of the uterus. Finally, the shifted-routing continuum manipulator is used to reach targets in a planner endometrium model. The experimental results show that the tip of the manipulator can reach all the area of endometrium from proper directions.**

I. Introduction

Intrauterine adhesion (IUA) is one of the main diseases that cause female infertility [1]. Endometrial regeneration using stem cells is a novel therapy for treating IUA. This treatment has the ability to fundamentally cure endometrial damage and restore fertility, but the success rate is strongly limited by current manual operation due to low accuracy of stem-cell transplantation [2,3]. Transplanting stem-cell into the native endometrium is considered as a procedure of *in situ* bioprinting. To successfully complete stem cell transplantation, there are two key steps: 1. Generate transplant wounds such as restoring uterine cavity structure, repairing injured endometrium and making Irritant injury. 2. Transplant stem cell to uterine cavity liking perfusion or injection stem cell solution [2]. However, the narrow cervical canal (4mm diameter [4]) confines the size of instruments for stem cell treatment. The uterine cavity, a mere slit which is flattened antero-posteriorly [5], requires instruments to be flexible enough to reach uterine wall from proper directions. As shown in Fig. 1, the operations on fundus require a manipulator to reach the endometrium in forward direction but the operations on corpus require the manipulator to reach the endometrium in lateral direction. The traditional hysteroscopy surgery instruments are hard and have low operation accuracy and poor dexterity. What's worse, these instruments will cause second damage to endometrium [6]. In this paper, we focus on the design of the continuum manipulator which is intended to perform the procedures of intra-lumenal *in situ* bioprinting to realize endometrium regeneration. In order to fit uterine cavity, the continuum robot is required to be with high dexterity but have small size and simple structure.

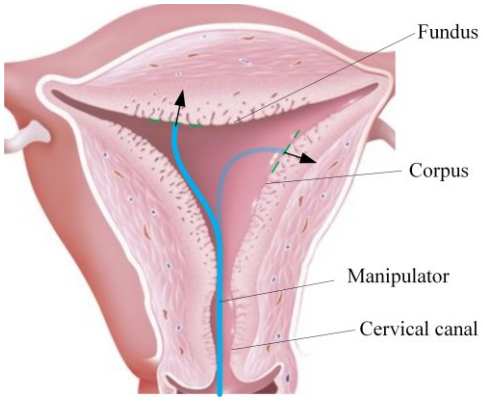

Fig. 1. A continuum robot reaches endometrium in uterine cavity with two different shapes. S-shape is feasible for the operation on fundus and C-Shape is feasible for the operation on corpus.

Continuum robots have been widely used to complete difficult operation in confined human lumens due to their advantages of flexibility and dexterity [7-9]. However, increasing the flexibility and dexterity of robots led to complicated structures, large number of actuations, and difficult control. Many continuum robots are designed to achieve great dexterous workspace while maintaining small size and simple structure. Some researchers increase the number of segments to improve the dexterity of continuum robots. A. Bajo *et al.* designed a dexterous 2-segment 5 DOFs continuum manipulator for minimally invasive surgery of the throat [10]. K. Xu *et al.* proposed 2-segment 6 DOFs continuum manipulators to perform single port laparoscopy [11]. These continuum robots have great dexterity but their large numbers of actuations led to complicated structures, big size and difficult control. R. J. Hendrick *et al.* designed concentric tube manipulators that consist of procurved and elastic tubes to remove prostate tissue in man urethra [12]. Besides, T. D. Nguyen *et al.* proposed a continuum robot with extensible segments to increase robot's workspace and

Resrach supported by National Natural Science Foundation of China (Grant No.61873257) and in part by the Youth Innovation Promotion Association CAS (Grant No.2020206).

J. Li, Y. Zhou and H. Liu are with State Key Laboratory of Robotics, Shenyang Institute of Automation, Chinese Academy of Sciences, Shenyang, 110016, China, Institutes for Robotics and Intelligent Manufacturing, Chinese Academy of Sciences, Shenyang, 110016, China, and also with Key Laboratory of Minimally Invasive Surgical Robot, Liaoning Province, Shenyang, 110016, China. Besides, J. Li is also with University of Chinese Academy of Sciences, Beijing 100049, China. (e-mail: lijianhua@sia.cn, zhouyuanyuan@sia.cn, Corresponding author e-mail: liuhao@sia.cn).

J. Tan is with Obstetrics and Gynecology Department, Assisted Reproduction Center, Shengjing Hospital affiliated to China Medical University, Shenyang, 110016, China. (e-mail: tjczjh@163,com).

Z. Wang is with the Department of Advanced Robotics, Chiba Institute of Technology, Narashino, Chiba, 275-0016, Japan (e-mail: zhidong wang@it-chiba.ac.jp.).

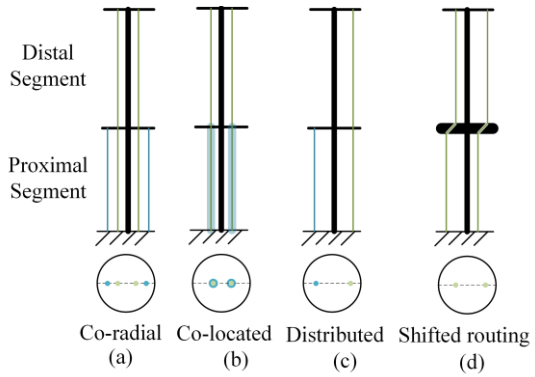

Fig. 2. Options for actuation routing. (a) and (b) require four tendons. (c) and (d) require two tendons.

dexterity [13]. However, these continuum robots are not feasible for endometrium generation surgery because it is not easy for them to provide channels for fiberscope and other instruments. In addition, some researchers strengthen dexterity and realize multiple bending forms of robots by making asymmetric backbone structure or contact points. A. Gao *et al.* designed a contacted-aided catheter to carry out the isolation operation in human heart [14]. K. Oliverbutler *et al.* created non-constant curvature bending manipulator by varying the notches in tubes [15]. When notches are rotated, s-shaped manipulators are created. Besides, some researchers improve continuum robots' dexterity by using different actuation methods. D. C. Rucker and A. Gao *et al.* designed helical tendons actuated continuum robots to realize robots' spatial shape and S shape [16,17]. In conclusion, many methods are proposed to enforce manipulators' dexterity, such as: increasing segments of robots, making asymmetric backbones, setting restricted structures, and changing actuator routing. Inspired by these works, we proposed a continuum manipulator which is actuated by shifted-routing cables for endometrium regeneration surgery. This continuum manipulator has advantages of concise structure and minimal actuation number. Though the continuum manipulator has only one section in the case of actuation structure, it can realize multiple shapes.

This paper is presented as following. First, a novel actuation routing is proposed and the design of the manipulator is introduced. Then, we present the kinematic model of the continuum manipulator. The dexterity analysis and theoretical evaluation are also presented. Finally, we experimentally validate the ability of the manipulator for reaching targets on fundus and corpus of uterus. The experimental results and conclusion are also presented.

II. Continuum Manipulator Design

A. Requirements

In endometrial regeneration surgery, the manipulator has to pass through cervix, whose diameter is usually 4 mm under nature condition, before it get uterine cavity and perform operation. This requires the manipulator's outer diameter to be smaller than 4 mm. On the other hand, to enable the manipulator to reach the whole uterine cavity, the manipulator should be with certain dexterity which allows operations on fundus and corpus of uterus. Besides, the manipulator should have two lumens for the deployment of fiberscope and other instruments. The design requirements are illustrated in Tab. I.

TABLE I. Design Specification

Specification	Value
Outer diameter	≤4mm
Types of shape	"C" shape & "S" shape
Length	≥30mm
Range of rotation	$-\pi/2 \sim \pi/2$
Number of lumen	2
Size of lumen	≥1.5mm

B. Design and Fabrication

In order to realize S-shape, continuum manipulators are usually designed to have two segments which are actuated by different tendons. The survey of [18] provides three options for actuation routing: co-radial, co-located, and distributed, as shown in Fig. 2. Co-radial enables every segment to have 2-Dof but needs at least 4 tendons for a planar 2-segment continuum robot. Similar with co-radial, co-located also needs 4 tendons and the two proximal tendons are made of hollow rod, like nitinol tube. Distributed actuation routing needs two tendons but led to a low dexterity for distal segment. As shown in Fig. 2(c), the distal segment can only bend left. What's worse, the shapes of distal segment are easily affected by external force since the segment is controlled by only one tendon. To overcome these disadvantages, we propose a new actuation routing, shifted-routing (Fig. 2(d)), to improve the manipulator's dexterity and stability.

A large number of tendons will limit the size of the manipulator and increase the complexity of actuation unit. Therefore, we design a continuum manipulator actuated by only two tendons, using the shifted-routing proposed above. The structure of the manipulator is shown in Fig. 3. The central backbone is a nitinol rode with n supporting disks spaced apart along its length. Two cable routings are

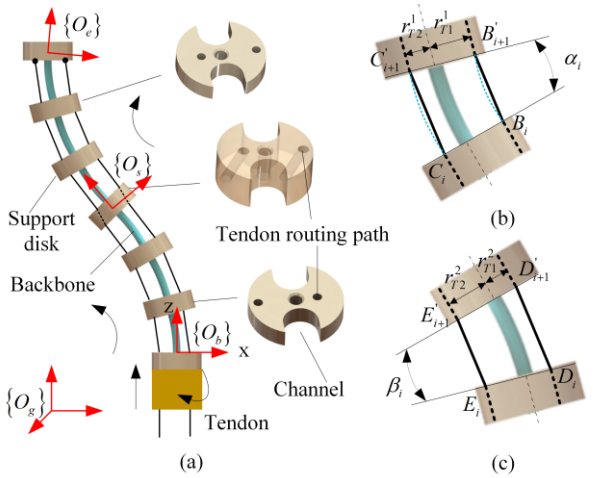

Fig. 3. Structure of continuum manipulator. (a) The structure and coordinate systems of the manipulator. (b) A flexible joint in distal segment. (c) A flexible joint in proximal segment.

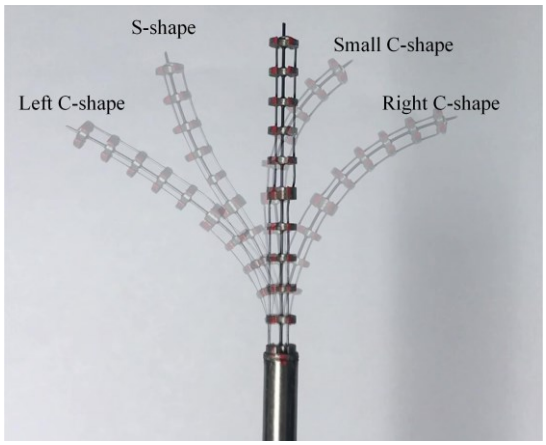

Fig. 4. Multiple shapes of the continuum manipulator.

distributed asymmetrically around the neutral axis of supporting disks. The cables can be pulled to deform the manipulator but they cannot allow pushing. Though the manipulator can be considered as having only one segment in the case of actuation structure, we also divide the manipulator into two segments for convenience. For proximal segment, the distance from the left cable routing to neutral axis is bigger than the distance from the right cable routing to neutral axis. For the distal segment, the case is converse. The middle support disk has two cant cable channels which tune the distance between cable and central axis. The multiple shapes of the manipulator are shown in Fig. 4. Besides, every support disk has two notches with the size of 1.5mm to provide channels for fiberscope and other instruments. These support disks can be easily made by metal 3D printing.

III. Modeling and Simulation

In this section, we derive the forward kinematics from configuration space to work space and the mapping from configuration space to joint space. Instead of considering every continuum segment as a constant curvature arc [18], we express the transformation matrix of every flexible joint and supporting disk according to the geometry of manipulator. The geometric constraints on cable displacement are also developed. Besides, the workspace and dexterity of the manipulator are explored and its ability of reaching the endometrium is also verified by simulation.

A. Kinematics of the Continuum Robot

First, we define the bending angle of a flexible joint as α_i, and then its homogenous transformation matrix can be expressed as

$$T_{\alpha_i} = T(\alpha_i) = \begin{bmatrix} \cos\alpha_i & 0 & \sin\alpha_i & \dfrac{l(1-\cos\alpha_i)}{\alpha_i} \\ 0 & 1 & 0 & 0 \\ -\sin\alpha_i & 0 & \cos\alpha_i & \dfrac{l\sin\alpha_i}{\alpha_i} \\ 0 & 0 & 0 & 1 \end{bmatrix} \quad (1)$$

where l is the length of the flexible joint. For the distal segment, the homogenous transformation matrix from $\{O_e\}$ to $\{O_s\}$ can be obtained as

$$^{S\alpha}_{Dis}T = \prod_{i=1}^{n}(T_{\alpha_i} \cdot T_h) \quad (2)$$

where n is the number of flexible joints of distal segment, T_h is the transformation of support disk and h is related with the height of disks. The position and orientation of end-effector frame in $\{O_g\}$ can be described by

$$^{Ori}_{Dis}T = T_d \cdot T_\phi \cdot \prod_{j=1}^{m}(T_{\beta_j} \cdot T_h) \cdot \prod_{i=1}^{n}(T_{\alpha_i} \cdot T_h) \quad (3)$$

where m is the number of flexible joints of proximal segment, T_ϕ is the transformation of robot rotation and T_d is the transformation of robot displacement. When the friction between cable and disks is small enough, the joint angles of a same segment are considered same. We define the configuration states as

$$\psi = [\alpha \ \ \beta \ \ \phi \ \ d] \quad (4)$$

where α is the bending angle of the distal segment and β is the bending angle of proximal segment. Next, we associate configuration parameters with actuation states. According to the arc geometry of flexible joints shown in Fig. 3 (b) and Fig. 3(c), the relation between joint angle and cable is expressed as

$$\begin{aligned} l_{B_{i+1}'B_i} &= 2\left(\frac{l}{\alpha_i} - r_{T1}^1\right)\sin\frac{\alpha_i}{2} \\ l_{C_{i+1}'C_i} &= 2\left(\frac{l}{\alpha_i} + r_{T2}^1\right)\sin\frac{\alpha_i}{2} \end{aligned} \quad (5)$$

and

$$\begin{aligned} l_{D_{i+1}'D_i} &= 2\left(\frac{l}{\beta_i} - r_{T1}^2\right)\sin\frac{\beta_i}{2} \\ l_{E_{i+1}'E_i} &= 2\left(\frac{l}{\beta_i} + r_{T2}^2\right)\sin\frac{\beta_i}{2} \end{aligned} \quad (6)$$

where r_{T1}^1, r_{T2}^1, r_{T1}^2 and r_{T2}^2 are the distances from tendon pathway to the central axis of disks. We simplify $\sin\frac{\alpha_i}{2}$ and $\sin\frac{\beta_i}{2}$ using Taylor series and then cable displacements are expressed as

$$\begin{aligned} \Delta l_{aT1} &= nr_{T1}^1\left(\alpha_i - \frac{\alpha_i^3}{3}\right) + mr_{T1}^2\left(\beta - \frac{\beta_i^3}{3}\right) + nl\frac{\alpha_i^2}{3} + ml\frac{\beta_i^2}{3} \\ \Delta l_{aT2} &= -nr_{T2}^1\left(\alpha_i - \frac{\alpha_i^3}{3}\right) - mr_{T2}^2\left(\beta - \frac{\beta_i^3}{3}\right) + nl\frac{\alpha_i^2}{3} + ml\frac{\beta_i^2}{3} \end{aligned} \quad (7).$$

Given the values of cable displacements, we can easily calculate the values of configuration parameters α and β by soling this equation.

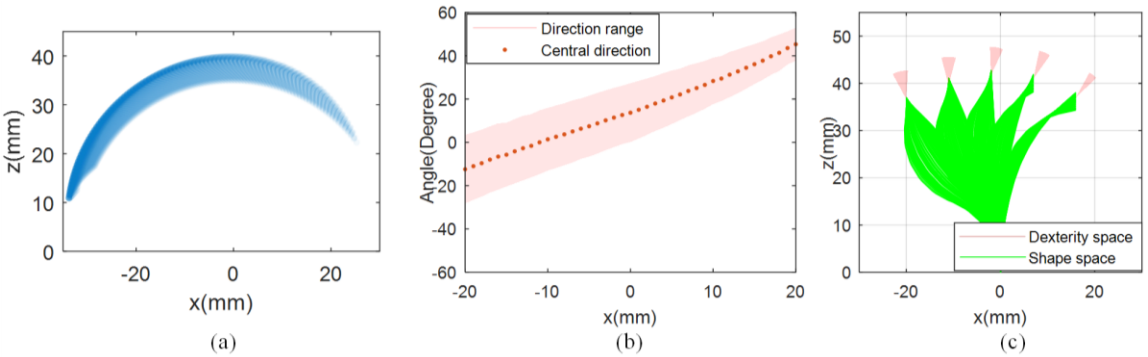

Fig.5. Workspace and dexterity analysis. (a) Workspace of the manipulator. (b) Dexterity along x- axis. (c) Some cases along x- axis

B. *Geometric Constrains*

To avoid collision of cables with backbone and protective layer, the bending angle of joints is confined by

$$\begin{aligned}(\frac{l}{\alpha}+r_{T2})\cos\frac{\alpha}{2}>\frac{l}{\alpha}\\(\frac{l}{\alpha}-r_{T1})\cos\frac{\alpha}{2}>(\frac{l}{\alpha}-R)\end{aligned} \tag{8}$$

where R is the radius of supporting disk. The maximal value and minimal value of bending angle are confined by the parameters of beam and cable routing path. The allowed strain of the backbone also provides limitation to the maximal value of bending angle. Besides, cable displacements are required to follow a principle that cables provide pull force but cannot provide thrust force. We consider the situation that robot is actuated by only one cable. According to the force balance of single joint, the bending angles of joint is expressed as

$$\begin{aligned}\frac{EI\alpha}{l}=T\cdot\cos\frac{\alpha}{2}\cdot r_T^1\\\frac{EI\beta}{l}=T\cdot\cos\frac{\beta}{2}\cdot r_T^2\end{aligned} \tag{9}$$

where E is the young's modulus if beam and I is the moment inertia of beam. Using the Taylor series of cosine, the relation between α and β is simplified as

$$r_T^1(\frac{1}{\alpha}-\frac{\alpha}{8})=r_T^2(\frac{1}{\beta}-\frac{\beta}{8}) \tag{10}$$

Finally, the displacement limitation of another cable is defined as

$$\Delta l_{\lim}=r_{T1}^1\sum(\alpha_i-\frac{\alpha_i^3}{3})+r_{T1}^2\sum(\beta_i-\frac{\beta_i^3}{3})+l\sum\frac{\alpha_i^2}{3}+l\sum\frac{\beta_i^2}{3} \tag{11}$$

This equation shows the minimal values of cable displacement of avoiding slack of cables.

C. *Workspace and Dexterity*

To investigate the reachability of end-effector, the workspace of continuum manipulator was scanned for $-1.5mm\le\Delta l_{aT1}\le 3mm$ and $-1.5mm\le\Delta l_{aT2}\le 3mm$. Note that the results didn't include the effect of rotation and translation in order to well show the bending freedom. The cases where cables get slack are excluded to maintain the feasibility under different cable displacements. Fig. 5(a) shows the achievable workspace under the limitation of cable displacements. The dexterous workspace of a manipulator is defined as the volume of space which can be reached by the manipulator with arbitrary orientation. Since the manipulator has a translation freedom along z-axis, we only investigate the dexterity of the manipulator along x-axis on a plane. Given a desired position in the x direction, we calculate the possible cable displacement by using Newton solver. 300 random initial inputs are used for every desired position. The dexterity of manipulator alone x-axis is shown in Fig. 5(b) and Fig. 5(c). The distal direction is defined as the angle between distal tip and z-axis.

The workspace and dexterity of the manipulator is unsymmetrical as a result of two shifted and dissymmetry cable routings. The manipulator has a large and concentrated left workspace and small right workspace. A large distal bending angle is useful for the operation on the corpus of uterus. In the left workspace, the central directions of dexterity space are near 0^o. It's favorable for the operation on the fundus of uterus. Therefore, the asymmetric workspace and dexterity make the continuum manipulator better fit the structure of uterine cavity though manipulator rotation is required to complete a three-dimensional workspace. In addition, we compare the dexterity along x-axis between shifted routing and distributed routing which are all actuated by two cables. The mean range of dexterous space along x-axis of shifted routing robot is 25.2^o and the mean range of dexterous space along x-axis of distributed routing robot is 24.7^o. Shifted

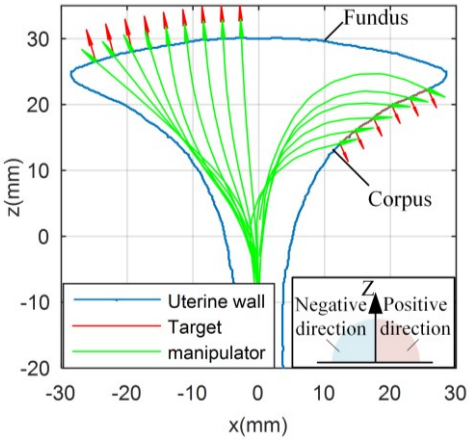

Fig. 6. Continuum manipulator reaches fundus and corpus of uterus in simulation.

routing slightly improved the dexterity of robot and it enhances the stability of distal segment as we mentioned in section II.

D. Simulation

To further explore the manipulator's ability, we investigate the manipulator's performance of reaching targets in simulation to show the benefit of this continuum manipulator. In endometrial regeneration surgery, the manipulator's tip is required to reach the endometrium from proper direction in order to successfully perform tasks like generating transplant wounds and transplanting stem cells. Besides, there is a limitation for the shapes of the manipulator that the conflict between endometrium and manipulator should be avoided. In the simulation, we construct a planar endometrial model and select some points as the targets. The desired direction is defined as same with the normal direction of the target endometrium. The actuation parameters are also solved by using locally convergent Newton solver. The simulation results are shown in Fig. 6. We see that the manipulator can successfully reach all the targets whether on the fundus or on the corpus. Though not all desired distal directions are achieved, all the arrows on the distal tip of the manipulator inserted into the uterine wall.

IV. Experiments

In this section, a prototype is made to evaluate the continuum manipulator's ability for endometrium surgery.

A. Experimental Setup

A continuum manipulator prototype was constructed and fixed on a 4 DOFs platform, shown in Fig. 7. The diameter of the manipulator is 3.9 mm. The deformation of the manipulator is driven by two 0.234-mm diameter core wire. The displacements from the tendon pathways to the central axis are separately 0.8 mm and 1.5 mm. Each wire terminated on a tension sensor (Bengbu Chino Sensor; CN). The two sensors were fixed on two linear sliders which were actuated by DC motors (E-Drive System 6200.T; CN). The rotation of the manipulator is driven by a pair of gears and the gears are

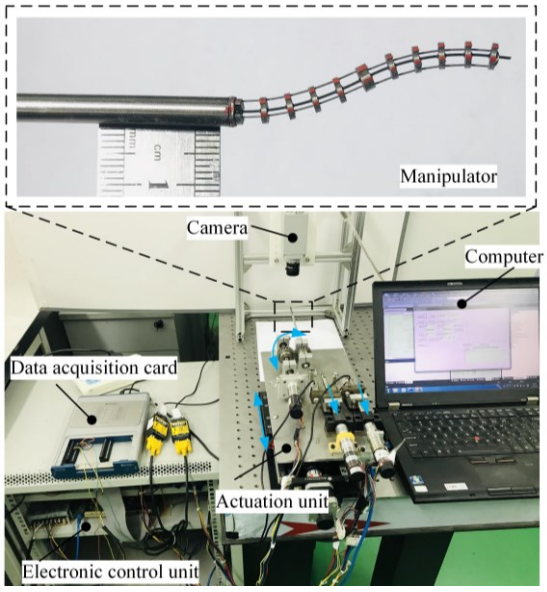

Fig. 7. Experimental setup

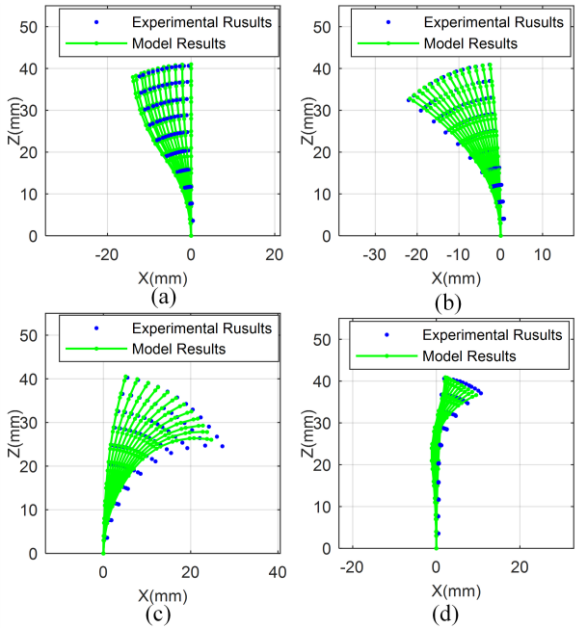

Fig. 8. Experimental results. (a) Reaching in forward direction when two cables were driven at the same time. (b) Left lateral direction with C-shape when left cable was driven to tension and right cable was driven to release. (c) Right lateral direction with big C-shape when right cable was driven to tension and left cable was driven to release. (d) Right lateral direction with small C-shape when right cable was driven to tension and left cable maintained still.

actuated by a DC motor (identical to those used for wire actuation). A servo-actuated carriage provided insertion movement. All DC motors were powered by drivers (Copley; USA) and controlled by a controller (Turbo Clipper; USA). A CMOS camera (PL-B776F, PixeLink, USA) was mounted over the manipulator to capture the shapes of manipulator during deformation.

B. Multiple Shapes in Freedom

The manipulator was separately actuated to reach in forward direction and lateral direction. First, two cables were driven at the same time with the same speed. Due to the shifted routing, the manipulator was actuated to S-shapes with forward direction. When the left cable was driven to tension and right cable was driven to release, the manipulator realized left C-shape. When the right cable was driven to tension while the left cable was release at the same time, the manipulator realized big C-shapes. However, when the right cable was driven to tension while the left cable maintains still, the manipulator realized small C-shapes. Assuming the elongation of cable is linear to cable tension, the actual cable displacement was calculated by removing the cable elongation from actuation displacements. The experimental results and model results are shown in Fig. 8. The distal position errors of the four situations are separately1.6±0.6mm, 0.3±0.2mm, 0.7±0.7mm, and 1.5±0.5mm. The distal direction errors of the four situations are separately 5.9±3.4°, 4.2±2.0°, 4.1±3.5°, and 4.2±3.5°.

C. Reaching Targets in Uterine Cavity

We experimentally evaluate the manipulator's ability of reaching targets. The angle between the manipulator's tip and the normal direction of target endometrium should be in the

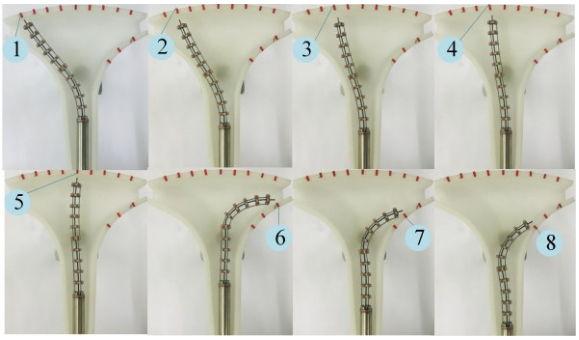

Fig. 9. Manipulator reaches the targets on fundus and corpus of uterus.

range of 0^o~90^o. In the experiments, a 2D model of uterine cavity was made. We selected 5 points spaced with 5mm on the fundus of uterus and 3 points space with 5mm on the corpus of uterus as the targets. The distal direction is defined as the angle between distal tip and z-axis, as shown in the subplot of Fig. 6. The reaching experiments were performed three times and the results are shown in Table II. The progress is shown in Fig. 9. When reaching targets on the fundus, the maximal deviation between distal direction and normal direction of the uterine wall is 21.1^o. When reaching targets on the corpus, the maximal deviation is 69.7^o. All targets can be reached from proper direction.

TABLE II. RESULTS OF REACHING TARGETS IN UTERINE CAVITY

	No.	Target direction (^{o})	Average values of achieved direction (^{o})	Deviation (^{o})
Operation on fundus	1	-11.8	-32.9	21.1
	2	-8.1	-16.0	7.9
	3	-5.7	-12.9	7.2
	4	-3.7	-4.5	0.8
	5	0.0	0.5	-0.5
Operation on corpus	6	153.0	83.3	69.7
	7	140.8	72.6	68.2
	8	126.3	66.1	60.2

V. CONCLUSION

In this paper, we present a novel shifted-routing cable-driven continuum manipulator with the advantages of high dexterity and simple structure which are essential for endometrium generation surgery. The shifted-routing actuation strategy needs less cables but show good dexterity. In experiments, we verified the manipulator's reaching ability in a 2D model of uterine cavity. The experimental results show that the manipulator can reach targets with proper direction (small than 70^o). However, we didn't consider the affection of the friction between cables and disks and ignored the compression of backbone, which will cause error between model results and experimental results. In our future work, we will consider these effectors and make a complete prototype in which a fiberscope and injection instruments are mounted. Additionally, the next step of our research is to use the continuum manipulator to perform the tasks of *in situ* bioprinting to realize endometrium regeneration in the future.

REFERENCES

[1] Y. Yu, L. Peng, L. Chen, L. Long, W. He, M. Li, and T. Wang, "Resilience and social support promote posttraumatic growth of women with infertility: The mediating role of positive coping," *Psychiatry research*, 2014, 215(2), pp. 401-405.

[2] C. B. Nagori, S. Y. Panchal, and H. Patel, "Endometrial regeneration using autologous adult stem cells followed by conception by in vitro fertilization in a patient of severe Asherman's syndrome," *Journal of Human Reproductive Sciences* 4.1(2011), pp. 43-8.

[3] J. Tan, P. Li, Q. Wang, Y. Li, X. Li, D. Zhang, and L. Kong, "Autologous menstrual blood-derived stromal cells transplantation for severe Asherman's syndrome," *Human Reproduction*, 31.12(2016), pp. 2723-2729.

[4] J. P. Nott, E. A. James, J. D. Pickering and N. A. Simpson, "The structure and function of the cervix during pregnancy," *Translational Research in Anatomy* 2.C(2016), pp. 1-7.

[5] Uterine cavity. (n. d.). In Wikipedia. Retrieved February 19, 2018 from https://en.wikipedia.org/wiki/Uterine_cavity

[6] Q. Wu, H. Xie, C. Ma, W. Zhang, Y. Liu and P. Liu, "Clinical Analysis of 767 Cases of Intrauterine Adhesions," J*ournal of Practical Obstetrics & Gynecology*, 2014, 30(05), pp. 354-357.

[7] J. Burgner-Kahrs, D. C. Rucker, H. Choset, "Continuum robots for medical applications: A survey," *IEEE Transactions on Robotics*, 2015, 31(6), pp. 1261-1280.

[8] N. Simaan, K. Xu, W. Wei, A. Kapoor, P. Kazanzides, R. Taylor and P. Flint, "Design and Integration of a Telerobotic System for Minimally Invasive Surgery of the Throat," *The International Journal of Robotics Research* 28.9(2009), pp. 1134-1153.

[9] J. Burgner, D. C. Rucker, H. B. Gilbert, P. J. Swaney, P. T. Russell, K. D. Weaver and R. J. Webster, "A telerobotic system for transnasal surgery," *IEEE/ASME Transactions on Mechatronics* 19.3 (2013), pp. 996-1006.

[10] A. Bajo, L. M. Dharamsi, J. L. Netterville, C. G. Garrett and N. Simaan, "Robotic-assisted micro-surgery of the throat: The trans-nasal approach," IEEE International Conference on Robotics and Automation. IEEE, 2013, pp. 232-238.

[11] K. Xu, J. Zhao and M. Fu, "Development of the SJTU unfoldable robotic system (SURS) for single port laparoscopy," *IEEE/ASME Transactions on Mechatronics*, 2015, 20(5), pp. 2133-2145.

[12] R. J. Hendrick, S. D. Herrell, and R. J. Webster, "A multi-arm hand-held robotic system for transurethral laser prostate surgery," IEEE international conference on robotics and automation (ICRA). IEEE, 2014, pp. 2850-2855.

[13] T. D. Nguyen and J. Burgner-Kahrs, "A tendon-driven continuum robot with extensible sections" 2015 IEEE/RSJ International Conference on Intelligent Robots and Systems (IROS). IEEE, 2015, pp. 2130-2135.

[14] A. Gao, H. Liu, Y. Zou, Z. Wang, M. Liang and Z. Wang, "A Contact-Aided Asymmetric Steerable Catheter for Atrial Fibrillation Ablation," *IEEE Robotics and Automation Letters* 2.3(2017), pp.1525-1531.

[15] K. Oliverbutler, Z. H. Epps and D. C. Rucker, "Concentric agonist-antagonist robots for minimally invasive surgeries," In Medical Imaging 2017: Image-Guided Procedures, Robotic Interventions, and Modeling, Vol. 10135, pp. 1013511..

[16] D. C. Rucker and R. J. Webster, "Statics and dynamics of continuum robots with general tendon routing and external loading," *IEEE Transactions on Robotics*, 2011, 27(6), pp. 1033-1044.

[17] A. Gao, H. Liu, Y. Zhou, Z. Yang, Z. Wang and H. Li, "A cross-helical tendons actuated dexterous continuum manipulator," 2015 IEEE/RSJ International Conference on Intelligent Robots and Systems (IROS). IEEE, 2015, pp. 2012-2017.

[18] R. J. Webster, and B. A. Jones, "Design and Kinematic Modeling of Constant Curvature Continuum Robots: A Review," *The International Journal of Robotics Research* 29.13(2010), pp. 1661-1683.